Journal of Alloys and Compounds 509 (2011) 2606–2610

Contents lists available at ScienceDirect

Journal of Alloys and Compounds

journal homepage: www.elsevier.com/locate/jallcom

Effect of isothermal annealing on the compressive strength of a ZrAlNiCuNb metallic glass

Min Song*, Yuehui He

State Key Laboratory of Powder Metallurgy, Central South University, Changsha 410083, China

ARTICLE INFO

Article history:
Received 25 September 2010
Received in revised form
12 November 2010
Accepted 15 November 2010
Available online 23 November 2010

Keywords:
Amorphous materials
Annealing
Mechanical properties

ABSTRACT

The effects of isothermal annealing on the microstructures and compressive strength of a $Zr_{56}Al_{10.9}Ni_{4.6}Cu_{27.8}Nb_{0.7}$ bulk metallic glass (BMG) have been studied using X-ray diffraction, scanning electron microscopy and compression tests. It has been shown that only structural relaxation happens during annealing at the temperature below T_g (glass transition temperature), while both structural relaxation and nanocrystallization happen during annealing at the temperature above T_g. Compression tests indicated that the strength of the BMG increases with annealing time at 437 °C up to 20 min, after which the strength starts to decrease. The strength evolution of the BMG with the annealing time is due to combined effects of the variations of the free volume and nanocrystals.

1. Introduction

Bulk metallic glasses (BMGs) have attracted extensive attentions due to their excellent mechanical properties [1–3]. However, BMGs usually do not show any plastic deformation after yielding because they fracture along highly localized shear bands. Recent investigations have shown that large plastic strains can be achieved if the primary shear bands can be branched into many tiny shear bands [4–8]. Thus, the plasticity of BMGs can be substantially improved if a highly localized shear process along a primary shear band is effectively hindered and branches out into a large number of uniformly distributed shear bands.

The introduction of crystalline second phase particles in the amorphous matrix is proved to be an effective way to improve the plasticity of BMGs [9–11]. Hays et al. [9,10] and Szuecs et al. [11] showed that micro-sized dendritic structure phase formed during solidification can substantially improve the plasticity of ZrTiNbCuNiBe metallic glasses by inhibiting the formation of macroscopic shear bands. However, using a similar method, Heilmaier [12] found that micro-sized second phase particles in a $Zr_{55}Cu_{30}Al_{10}Ni_5$ metallic glass will degrade both the strength and plasticity due to the brittleness of the second phase particles. Previous studies [6,8,13,14] also indicated that dispersions of embedded nanocrystals (formed during annealing) are also thought to be effective for enhancing the mechanical properties of BMGs. It is believed that both the type and volume fraction of the crystalline phases have important effects on the mechanical properties of the metallic glasses. Up to now, limited data are available on the effect of second phase particles on the strength of the metallic glasses. In this paper, a $Zr_{56}Al_{10.9}Ni_{4.6}Cu_{27.8}Nb_{0.7}$ metallic glass was successfully fabricated by arc melting technique plus copper mold casting. The metallic glass was annealed under a vacuum condition to form nanocrystals in the amorphous matrix, and the effect of annealing on the compressive strength of the metallic glass was investigated.

2. Experimental

$Zr_{56}Al_{10.9}Ni_{4.6}Cu_{27.8}Nb_{0.7}$ alloy ingots were prepared by arc melting high-purity Zr (>99%), Cu (>99.9%), Ni (>99.9%) and Al (>99.9%) under an argon atmosphere. The ingot was remelted four times to ensure its microstructural homogeneity and then cast into a copper mold to produce a 70 mm long cylindrical rod with a diameter of 3 mm. X-ray diffraction pattern (Dmax 2500VB) showed that the obtained material has a complete amorphous structure (not show here). Thermal properties associated with glass transition and crystallization temperatures were evaluated by differential scanning calorimeter (DSC, NETZSCH 204) with a heating rate of 20 K per minute. The glass was then annealed from 5 min to 120 min at different temperatures under a vacuum condition to form nanocrystals in the amorphous matrix. The structures of the samples after annealing were examined by X-ray diffraction (Dmax 2500VB) and scanning electron microscope (SEM, FEI Sirion 200). Uniaxial compression tests were performed on the annealed and un-annealed samples at a quasi-static strain rate of 10^{-6} s^{-1} in an Instron 3369 testing machine using rod samples with 3 mm in diameter and 6 mm in length. All the compression tests were repeated 3–5 times to ensure the data accuracy. The fracture surfaces of the specimens after compression were examined using scanning electron microscopy (SEM, FEI Nano 230).

* Corresponding author. Tel.: +86 731 88877880; fax: +86 731 88710855.
E-mail address: Min.Song.Th05@Alum.Dartmouth.ORG (M. Song).

0925-8388/$ – see front matter © 2010 Elsevier B.V. All rights reserved.
doi:10.1016/j.jallcom.2010.11.114

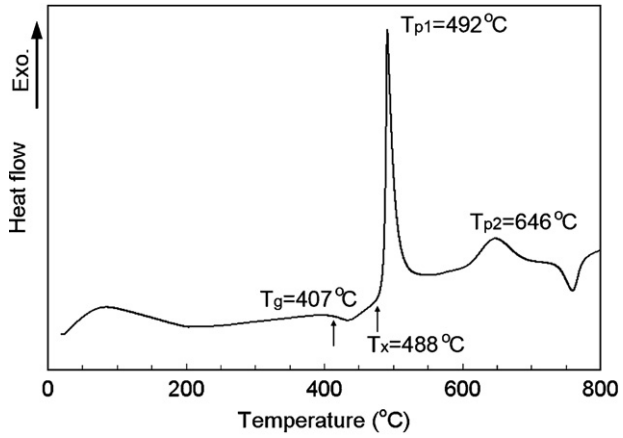

Fig. 1. DSC curve of the specimen, with a heating rate of 20 K per minute.

3. Results

3.1. DSC curve

Fig. 1 shows the DSC curve of the prepared $Zr_{56}Al_{10.9}Ni_{4.6}Cu_{27.8}Nb_{0.7}$ bulk metallic glass. It can be seen that the glass transition temperature (T_g, glass transition temperature) and crystallization temperature (T_x, crystallization temperature) are 407 °C and 488 °C, respectively. Two crystallization peaks are detected by DSC examination, with the peak temperature being around 492 °C (T_{p1}) and 646 °C (T_{p2}), respectively. It should be noted that T_{p1} and T_{p2} are related to the crystallization temperatures of different crystalline phases (might be Al_3Zr, $Al_5Zr_3Ni_2$ or other phase based on X-ray diffraction pattern as shown in Fig. 2). Based on the DSC examination results, a serial of the temperatures, below T_g, between T_g and T_x, and above T_x, were chosen as the annealing temperatures to see how the annealing temperature affects the crystallization behavior.

3.2. X-ray diffraction patterns and distribution of the nanocrystals

Fig. 2a shows the X-ray diffraction patterns of the $Zr_{56}Al_{10.9}Ni_{4.6}Cu_{27.8}Nb_{0.7}$ bulk metallic glass after annealed for 20 min at different temperatures. It can be seen that when the annealing temperature (250 °C and 337 °C) is below T_g, the annealed specimens still show the broad diffraction halo that is typical of the amorphous structure. This means that the samples annealed below T_g for 20 min in this study are overall amorphous within the detection limit of XRD. It can also be seen that when the annealing temperature (437 °C and 517 °C) is above T_g, crystalline second phases are formed in the amorphous matrix after annealed for 20 min, since diffraction peaks can be clearly observed. This means that the samples can nucleate crystalline second phases if the annealing temperature is above T_g in this study. Indexing of the diffraction peaks indicated that the main crystalline phases include face-centered cubic Al_3Zr, $Al_5Zr_3Ni_2$ and an unknown phase. Fig. 2b shows the X-ray diffraction patterns of the $Zr_{56}Al_{10.9}Ni_{4.6}Cu_{27.8}Nb_{0.7}$ bulk metallic glass after annealing to different times at a temperature of 437 °C. It can be seen that crystalline second phases are formed in the amorphous matrix for all the annealing time, and the crystalline degree increases with increasing the annealing time since the height of the X-ray diffraction peaks increase with the annealing time. The main crystalline phases are also Al_3Zr, $Al_5Zr_3Ni_2$ and an unknown phase.

Fig. 3 shows the SEM micrographs of the specimens after annealing for 5, 20 and 60 min at a temperature of 437 °C. It can be seen from Fig. 3(a) that very few second phase particles can be observed in the amorphous matrix after annealed for 5 min, while it can also be seen from Fig. 3(b) and (c) that numerous spherical second phase particles distribute uniformly in the amorphous matrix after annealed for 20 and 60 min, with the average size of the particles being 5–10 nm and 10–20 nm, respectively.

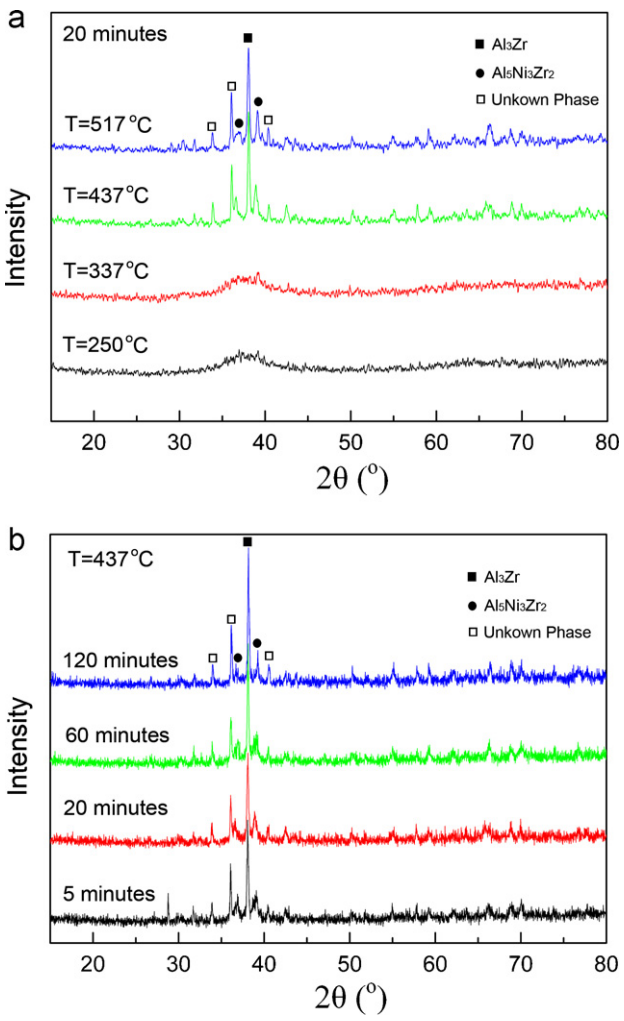

Fig. 2. X-ray diffraction patterns of the specimen after annealed (a) at different temperatures for 20 min and (b) for different periods at 437 °C.

3.3. Compression behaviors

Fig. 4a shows typical compressive strength/displacement curves of the $Zr_{56}Al_{10.9}Ni_{4.6}Cu_{27.8}Nb_{0.7}$ bulk metallic glass after annealed for various periods at 437 °C, together with the data of the metallic glass without annealing. It can be seen from Fig. 4a that the glass deforms elastically and fractures without any plasticity, no matter how long the glass was annealed. This means that annealing cannot improve the plasticity of the $Zr_{56}Al_{10.9}Ni_{4.6}Cu_{27.8}Nb_{0.7}$ bulk metallic glass. On the other hand, it can be seen from Fig. 4a and b that the maximum strength increases initially from 1597 MPa before annealing to 1945 MPa after annealed for 20 min, after which the maximum strength starts to decrease. This phenomenon indicates that there is an ideal annealing time, at which the metallic glass can achieve the maximum strength.

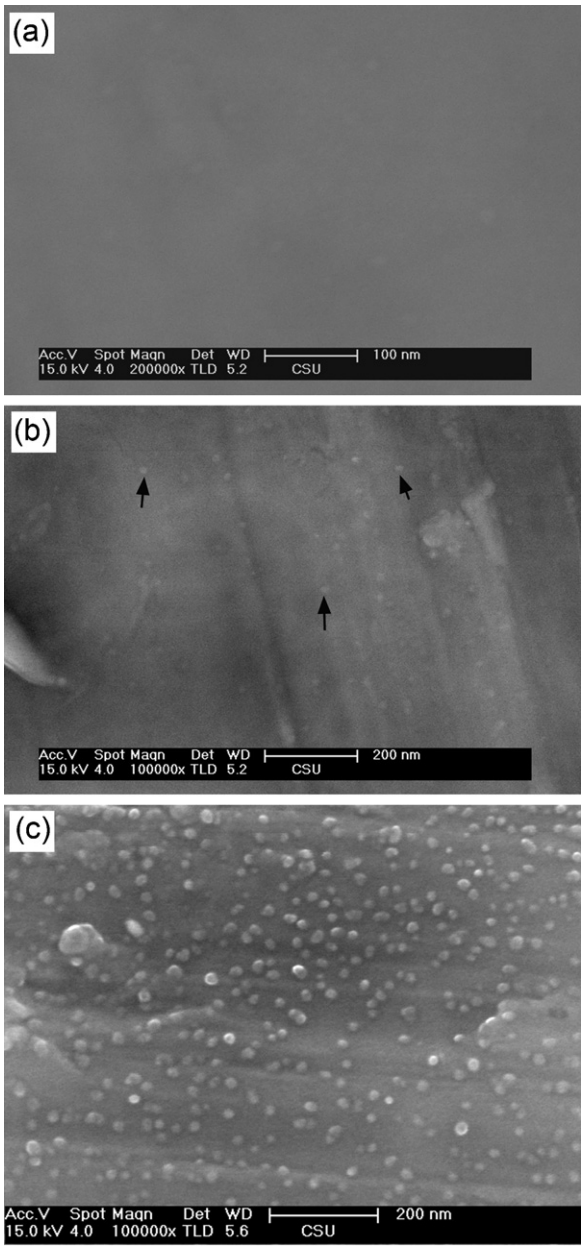

Fig. 3. SEM micrograph of the specimen after annealed for (a) 5, (b) 20 and (c) 60 min at a temperature of 437 °C.

3.4. Fracture surfaces

The variation of the strength during annealing can be verified through observing the fracture surface micrographs of the $Zr_{56}Al_{10.9}Ni_{4.6}Cu_{27.8}Nb_{0.7}$ bulk metallic glass after compression tests. Fig. 5a shows the SEM fracture surface micrograph of the metallic glass without annealing. The fracture surface is similar to many previous studies [15,16], in which the vein-like pattern in the fracture surface are clearly observed. The formation of the vein-like pattern may be attributed to the larger viscosity of the $Zr_{56}Al_{10.9}Ni_{4.6}Cu_{27.8}Nb_{0.7}$ BMG, and it indicates an instantaneous shear fracture. Fig. 5b shows the SEM fracture surface micrograph of the BMG after annealed for 20 min. It can be seen from Fig. 5b that dense multiple primary and secondary shear bands can be achieved, indicating stable propagation of the shear bands during compression. The width of a single shear band is in the range of several nanometers, which is similar to the size of the annealing nucleated second phase particles, as shown in Fig. 3(b). Fig. 5c shows the SEM fracture surface micrograph of the BMG after annealed for 60 min. It can be seen from Fig. 5c that the BMG fractures by cleavage along the shear plane, similar to most brittle materials such as rocks and intermetallics. This phenomenon indicates a low plasticity and strength of the material.

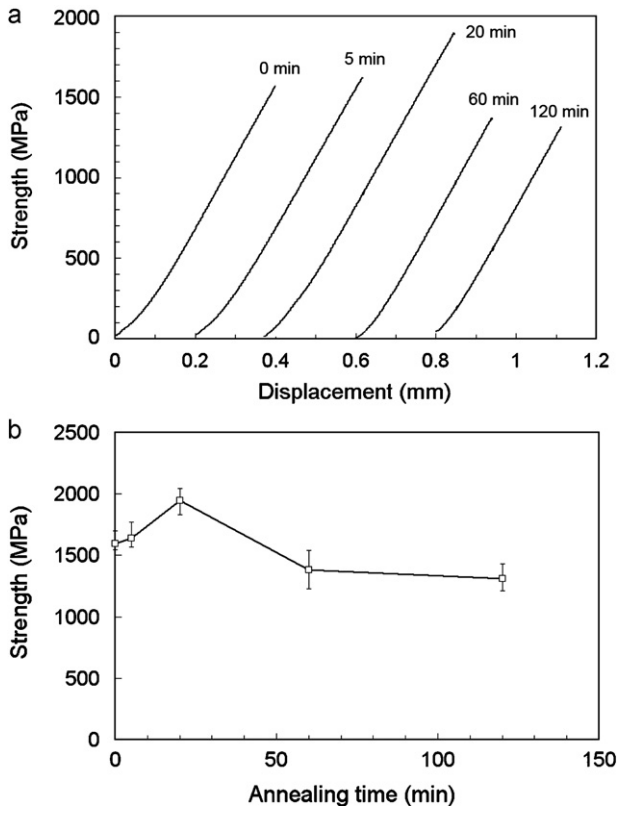

Fig. 4. (a) Compressive strength/displacement curves and (b) relationship between the maximum strength and annealing time of the metallic glass. Note that the annealing temperature is 437 °C.

4. Discussion

It can be seen from Fig. 2a that when the annealing temperature is below the T_g the annealed specimens still show the broad diffraction halo that is typical of the amorphous structure. This indicates that crystallization is very difficult at such a low temperature because the formation of crystalline second phase particles require atom diffusion, which is controlled by the annealing temperature and time. The most important feature during annealing at low temperature below T_g is the structural relaxation process, resulting in the reduction in the free volume and free energy. It can also be seen from Figs. 2 and 3 that when the annealing temperature is above T_g, crystalline second phase particles are formed in the amorphous matrix due to the high crystallization driving force and atom diffusion rate. One should be noted that at all temperatures above the room temperature, the structural relaxation process will happen to decrease the free volume and free energy. The higher is the annealing temperature and the longer is the annealing time, the less is the free volume in the matrix.

According to the phase mixture model [17], the compressive fracture strength of the metallic glass after annealing can be expressed as [17]:

$$\sigma = V_{\text{relax}}\sigma_{\text{relax}} + V_{\text{n}}\sigma_{\text{n}} \quad (1)$$

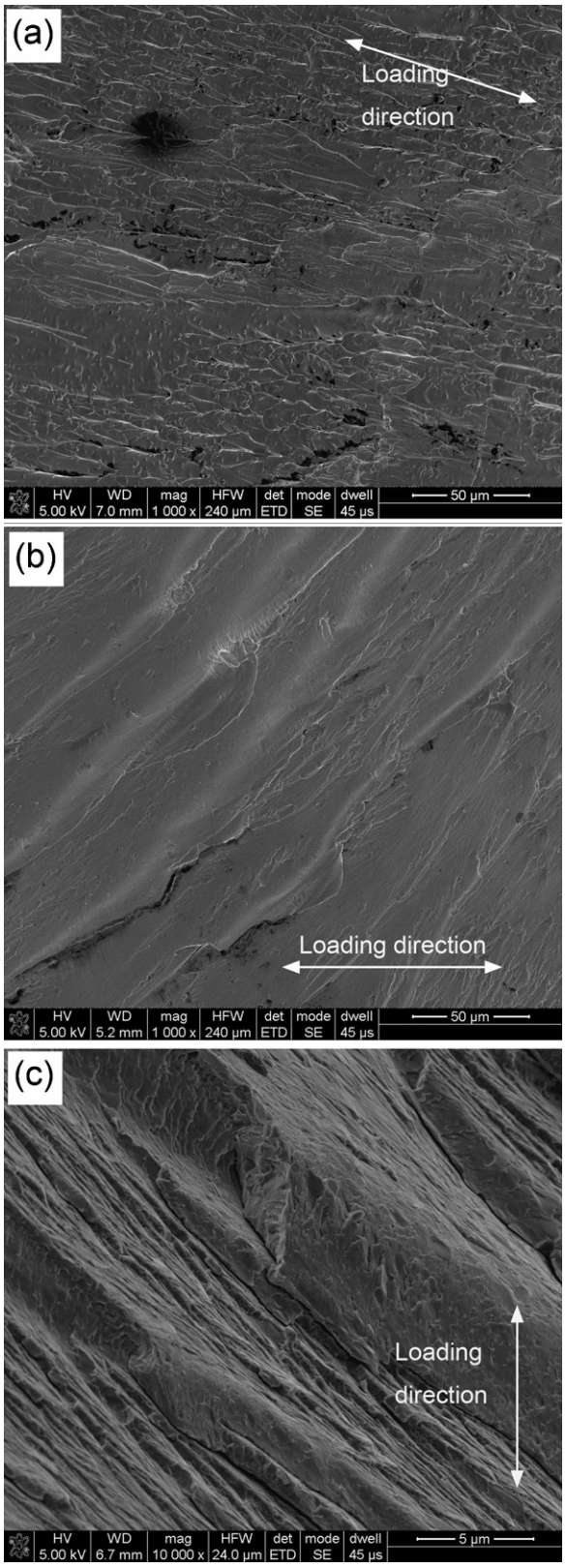

Fig. 5. SEM fracture surface micrographs of the $Zr_{56}Al_{10.9}Ni_{4.6}Cu_{27.8}Nb_{0.7}$ bulk metallic glass (a) without annealing, (b) after annealed for 20 min and (c) after annealed for 60 min.

where V_{relax} and V_n are the volume fractions of the amorphous matrix and nanocrystals, σ_{relax} is the fracture strength of the amorphous matrix in the relaxed state (after annealing) and σ_n is the fracture strength of the nanocrystals. According to the previous studies [18,19], the nanocrystals with the size less than 10 nm in the amorphous matrix have very high strength due to the perfect structures without defects. The size of these nano-particles is smaller than the width of the shear bands, and thus these particles cannot effectively inhibit the propagation of the shear bands and generate new secondary shear bands. On the other hand, these particles can inhibit the atom movements in the shear bands and decrease the width of the shear bands [20], and thus can improve the strength, similar to dispersed strengthening mechanism in the crystalline materials. Thus, the fracture strength increases initially with the annealing time up to 20 min since the volume fraction and size of the nanocrystals increase with the annealing time. It should be noted, however, once the annealing time is too long, the size and volume fraction of the nanocrystals increase too much, and the interspacing between the nano-particles decreases dramatically. These large and high volume fractioned second phase particles can severely inhibit the propagation of the shear bands and generate cracks at a rather low externally applied stress [19]. At that condition, the strength of the metallic glasses will be substantially decreased due to the fast propagation of the cracks, which are nucleated along the interface between the amorphous matrix and nanocrystals due to the high stress concentration.

It is generally accepted that flow in metallic glass involves the stress induced cooperative rearrangement of small groups of atoms referred to as shear transformation zones [21,22]. These shear transformation zones are associated with free volume. Annealing will result in the reduction in free volume, and thus in the decrease in the strength of the metallic glass [23]. Thus, it is believed that there is an ideal annealing time at a given temperature, in which the annealed BMGs have the maximum strength. Before the ideal annealing time, the decrease in the strength caused by the reduction in the free volume can be compensated by the nanocrystals formed in the amorphous matrix during annealing. While after the ideal annealing time, too less free volume will result in the decrease in the strength. Previous study [18] also indicated that an optimum volume fraction of nanocrystallization is beneficial for the strength in BMGs [18]. Consider that if the flow of newly formed shear bands by nanocrystals would be hindered by the closely spaced other nanocrystals, the strength would be degraded with excess nanocrystallization.

In the present work, the strength of the $Zr_{56}Al_{10.9}Ni_{4.6}Cu_{27.8}Nb_{0.7}$ bulk metallic glass increases during isothermal annealing up to 20 min, after which the strength starts to decrease. From Figs. 2 and 3, we know that the nanocrystals are formed during isothermal annealing at 437 °C, and that the crystallization degree increases with the annealing time. On the other hand, the reduction of the free volume during annealing results in the decrease in the nucleation rate of the shear bands, and thus decreases the strength. These two affecting factors result in the maximum value in the strength at about 20 min, at which the dense primary and secondary shear bands can clearly be observed on the fracture surface, as shown in Fig. 5b. Once the annealing temperature is above 20 min, the free volume is too less to nucleate enough shear bands for the deformation. At the same time, high volume fraction of the nanocrystals also facilitates the formation of interfacial voids during compression, resulting in a substantial decrease in the strength of the metallic glass, a phenomenon being also observed by Heilmaier [12], who also used a Zr based bulk metallic glass with similar composition to our material ($Zr_{55}Al_{10}Ni_5Cu_{30}$, without Nb addition) as the testing material. At that condition, the BMG fractures by cleavage along the shear plane, accompanied by low strength. It should

be noted that the addition of minor Nb can improve the glass formation ability and the fracture strength of Zr-based metallic glasses.

5. Conclusion

In this paper, a $Zr_{56}Al_{10.9}Ni_{4.6}Cu_{27.8}Nb_{0.7}$ BMG was prepared by arc melting technique. The effects of isothermal annealing on the microstructures and strength of the BMG have been studied using X-ray diffraction, SEM and compression tests. It has been shown that only structural relaxation process happens during annealing at a temperature below T_g, while both structural relaxation and nanocrystallization happen during annealing at a temperature above T_g. Compression tests indicated that the strength of the BMG increases with annealing time at 437 °C up to 20 min, after which the strength starts to decrease. Before 20 min, the decrease in the strength caused by the reduction in the free volume can be compensated by the nanocrystals formed in the amorphous matrix, and thus improving the strength. While after 20 min, the strength will be substantially decreased due to the fast propagation of the cracks, which are nucleated along the interface between the amorphous matrix and nanocrystals due to the high stress concentration.

Acknowledgements

This work is supported by China–Australia Special Fund (51011120053), National Natural Science Foundation of China (50823006 and 50825102), and Chinese Postdoctoral Science Foundation (200801345).

References

[1] A.L. Greer, Science 267 (1995) 1947.
[2] W.H. Wang, Prog. Mater. Sci. 52 (2007) 540.
[3] W.H. Wang, C. Dong, C.H. Shek, Mater. Sci. Eng. R 44 (2004) 45.
[4] K. Mondal, T. Ohkubo, T. Mukai, K. Hono, Mater. Trans. 48 (2007) 1322.
[5] D.S. Sung, O.J. Kwon, E. Fleury, K.B. Kim, J.C. Lee, D.H. Kim, Y.C. Kim, Met. Mater. Int. 10 (2004) 575.
[6] A. Inoue, W. Zhang, T. Tsurui, A.R. Yavari, A.L. Greer, Philos. Mag. Lett. 85 (2005) 221.
[7] J. Schroers, W.L. Johnson, Phys. Rev. Lett. 93 (2004) 255506.
[8] J. Das, M.B. Tang, K.B. Kim, R. Theissmann, F. Baier, W.H. Wang, J. Eckert, Phys. Rev. Lett. 94 (2005) 205501.
[9] C.C. Hays, C.P. Kim, W.L. Johnson, Phys. Rev. Lett. 84 (2000) 2901.
[10] C.C. Hays, C.P. Kim, W.L. Johnson, Mater. Sci. Eng. A 304–306 (2001) 650.
[11] F. Szuecs, C.P. Kim, W.L. Johnson, Acta Mater. 49 (2001) 1507.
[12] M. Heilmaier, J. Mater. Proc. Technol. 117 (2001) 374.
[13] H. Kato, K. Yubuta, D.V. Louzguine, A. Inoue, H.S. Kim, Scripta Mater. 51 (2004) 577.
[14] J.C. Lee, Y.C. Kim, J.P. Ahn, H.S. Kim, S.H. Lee, B.J. Lee, Acta Mater. 52 (2004) 1525.
[15] Z.F. Zhang, J. Eckert, L. Schultz, Acta Mater. 51 (2003) 1167.
[16] Z. Bian, G.L. Chen, G. He, X.D. Hui, Mater. Sci. Eng. A 316 (2001) 135.
[17] H.S. Kim, M.B. Bush, Y. Estrin, Mater. Sci. Eng. A 276 (2000) 175.
[18] C. Fan, C. Li, A. Inoue, V. Haas, Phys. Rev. B 61 (2000) 3761.
[19] K. Monda, T. Ohkubo, T. Toyama, Y. Nagai, M. Hasegawa, K. Hono, Acta Mater. 56 (2008) 5329.
[20] Z. Bian, G. He, G.L. Chen, Scripta Mater. 46 (2002) 407.
[21] F. Spaepen, Acta Metall. 25 (1977) 407.
[22] A.S. Argon, Acta Metall. 27 (1979) 47.
[23] N. Nagendra, U. Ramamurty, T.T. Goh, Y. Li, Acta Mater. 48 (2000) 2603.